Journal of Organometallic Chemistry 880 (2019) 312–316

Contents lists available at ScienceDirect

Journal of Organometallic Chemistry

journal homepage: www.elsevier.com/locate/jorganchem

Synthesis and structure of bis(indenyl)-rhodium and -iridium complexes

Vladimir B. Kharitonov [a], Yulia V. Nelyubina [a, b], Irina D. Kosenko [a], Dmitry A. Loginov [a, *]

[a] A. N. Nesmeyanov Institute of Organoelement Compounds, Russian Academy of Sciences, ul. Vavilova 28, 119991, Moscow, Russia
[b] Kurnakov Institute of General and Inorganic Chemistry, Russian Academy of Sciences, Leninskii prosp. 31, Moscow, 117901, Russia

ARTICLE INFO

Article history:
Received 26 September 2018
Received in revised form
7 November 2018
Accepted 20 November 2018
Available online 22 November 2018

Dedicated to the 70th anniversary of Prof. Armando J.L. Pombeiro in recognition of his great contribution to the organometallic chemistry.

Keywords:
Indenyl complexes
Iridium
Rhodium
Sandwich compounds

ABSTRACT

Bis(indenyl)-rhodium and -iridium complexes [(η^5-indenyl)M(η^5-$C_9H_2R_5$)]PF_6 (**2a**: M = Rh, R = H; **2b**: M = Ir, R = H; **3**: M = Rh, R = Me) were synthesized by reactions of iodides [(η^5-indenyl)MI_2]$_n$ (**1a**,**b**) with indenes in the presence of $AgPF_6$. The structures of **2a**SbF_6 and **2b**PF_6 were determined by X-ray diffraction. They have fully eclipsed geometry, in which the bridgehead carbon atoms of the indenyl ligands are arranged close to each other. Experimental and DFT calculation data showed that the strength of the M–indenyl bond in the bis(indenyl) compounds decreases in the following row: Ir > Co > Rh.

1. Introduction

The indenyl complexes of transition metals have found a wide range of applications in catalysis [1]. In particular, rhodium and iridium derivatives proved to be effective catalysts for cyclotrimerization of alkynes [2], dehydrogenation of alkanes and alcohols [3], hydroboration of olefins [4], amination of carbonyl compounds [5], as well as diverse C–H activation processes [6]. Such catalytic versatility is attributed to easy appearance of free coordination site at metal atom as a result of slippage of the indenyl ligand from η^5 to η^3 coordination mode (indenyl effect) [7]. The main driving force of this transformation is recovery of the benzene ring aromaticity.

After discovery of ferrocene in 1951 [8], it has attracted the attention of chemists in the preparation of sandwich compounds of other transition metals. In particular, rhoda- and iridacenium cations $[MCp_2]^+$ (M = Rh, Ir) have been synthesized by the reaction of metal acetylacetonates with CpMgBr [9]. The synthesis of bis(indenyl) metal complexes is an another challenge. Thus, the iron [10], cobalt [10a,c,e, 11], nickel [10c, 12], ruthenium [13], and osmium [14] derivatives as well as their X-ray structures (with exception of osmium) have been reported (Fig. 1). To the best of our knowledge, the parent bis(indenyl) complexes of rhodium and iridium [M(η^5-indenyl)$_2$]$^+$ (M = Rh, Ir) remain unknown. Only accidental formation of the bis(indenyl) rhodium moiety in 4% yield has been found in the reaction of [(η^5-indenyl)$RhCl_2$]$_n$ with Tl[Tl(η-7,8-$C_2B_9H_{11}$)] [15].

Herein we report a general synthetic approach to the bis(indenyl) complexes of rhodium and iridium as well as their X-ray structures.

2. Results and discussion

Recently, we have found that abstraction of iodides from the half-sandwich complexes [(η^5-indenyl)MI_2]$_n$ (M = Rh, Ir; **1a**,**b**) in the presence of benzene and its derivatives leads to the arene complexes [(η^5-indenyl)M(arene)]$^{2+}$ [5c, 16]. In the present work, we used this approach for synthesis of bis(indenyl) complexes. Thus, the reaction of **1a**,**b** with indene and $AgPF_6$ gives complexes [M(η^5-indenyl)$_2$]PF_6 (**2a**,**b**PF_6) in 70–75% yield (Scheme 1). The

* Corresponding author.
E-mail address: dloginov@ineos.ac.ru (D.A. Loginov).
URL: http://www.ineos.ac.ru/en

https://doi.org/10.1016/j.jorganchem.2018.11.027
0022-328X/

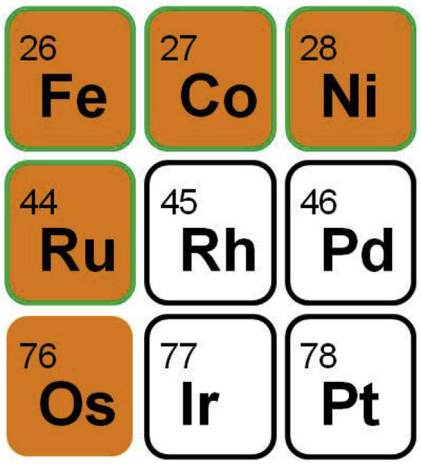

Fig. 1. Availability of bis(indenyl) complexes for Group 8, 9 and 10 elements. Orange background corresponds to elements, for which bis(indenyl) complexes are known (green borders – with X-ray structures); colorless background – bis(indenyl) complexes are unknown. (For interpretation of the references to color in this figure legend, the reader is referred to the Web version of this article.)

same reaction of **1a** with 1,2,3,4,7-pentamethylindene allowed us to prepare the asymmetrical rhodium complex [(η^5-indenyl)Rh(η^5-$C_9H_2Me_5$)]PF_6 (**3**PF_6) but in lower yield (33%). Interestingly, the reaction of iridium derivative **1b** with 1,2,3,4,7-pentamethylindene did not give any sandwich products that may be explained by steric hindrance of methyl groups. Probably, these reactions proceed via initial formation of the arene complexes [(η^5-indenyl)M(η^6-indene)]$^{2+}$, which are unstable and transform into the bis(indenyl) cations **2a**,**b** and **3** as a result of spontaneously deprotonation and $\eta^6 \rightarrow \eta^5$ haptotropic rearrangement. Unfortunately, we were unable to clearly detect the intermediates by ^{1}H NMR spectroscopy due to their complicated spectra (see Supporting Information). Nevertheless, the related rearrangement was observed earlier by Maitlis with coworkers for the reaction of the cyclopentadienyl complexes [Cp*M(Me_2CO)$_3$]$^{2+}$ (M = Rh, Ir) with indene [17]. Noteworthy, attempts to prepare cations **2a**,**b** by direct reactions of lithium indenide with **1a**,**b** or metal chlorides MCl_3 were unsuccessful.

Complexes **2a**,**b**PF_6 and **3**PF_6 are the first examples of the rhodium and iridium bis(indenyl) sandwich compounds. They are air-stable solids. In the ^{1}H NMR spectra of **2a**,**b**, the only one set of signals of the indenyl ligand (four multiplets) was observed in

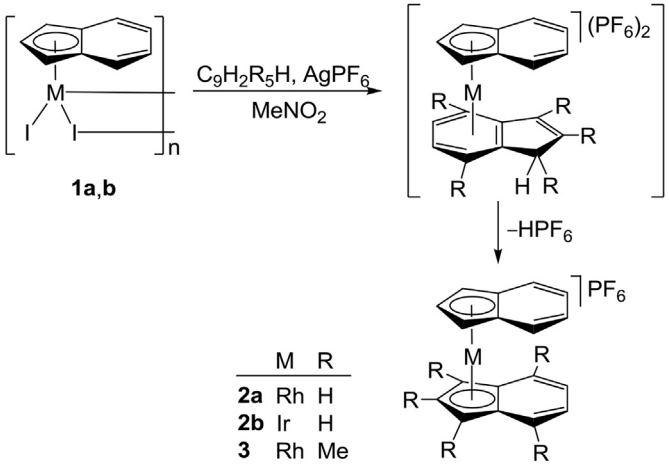

Scheme 1. Synthesis of the bis(indenyl) complexes **2a**,**b**PF_6 and **3**PF_6.

accordance with high symmetry of their structure. Noteworthy, the chemical shifts do not significantly depend on the metal nature. In contrast, in the ^{13}C NMR spectra of **2a**,**b** and the related cobalt derivative [Co(η^5-indenyl)$_2$]$^+$ the chemical shifts of coordinated carbon atoms are decreased in the sequence **2a** (av. 89.1 ppm) > [Co(η^5-indenyl)$_2$]$^+$ (av. 86.0 ppm) [18] > **2b** (av. 82.4 ppm) that correlates well with calculated dissociation energies (D_e) for the M–indenyl bond (Table 1) [19]. Earlier, Kohler stated a correlation between the ^{13}C NMR chemical shift of the indenyl bridgehead carbons and the hapticity of the coordinated indenyl ligand [18]. We found that the loosening of the Rh–indenyl bond as compared with the Co–indenyl bond is mainly caused by the increase of Pauli repulsion (ΔE_{Pauli}) because the attractive interactions (ΔE_{orb} and ΔE_{elstat}) remain unchanged. In the case of the Ir–indenyl bond, the increase of ΔE_{Pauli} is overruled by considerable increase of ΔE_{orb} and ΔE_{elstat} that thereby leads to increase of D_e.

As shown in Table 2, the ^{13}C NMR chemical shifts, calculated at the BP86/TZP level, are in a very good agreement with experimental values. For example, the calculated chemical shifts of coordinated carbon atoms are decreased in the same sequence: **2a** (av. 89.1 ppm) > [Co(η^5-indenyl)$_2$]$^+$ (av. 84.1 ppm) > **2b** (av. 81.0 ppm).

The structures of **2a**SbF_6 and **2b**PF_6 were determined by X-ray diffraction (Figs. 2 and 3). Cations **2a** and **2b** are "true" η^5-coordinated indenyl complexes; the slip parameters [20,10c,16] are rather low and equal to 0.043 and 0.052 Å, respectively. The planes of indenyl ligands are approximately parallel; the dihedral angles C_5/C_5 are equal 0.4 and 2.8°. At the same time, indenyl ligands are not almost planar and folded along the C8–C9 bond towards the metal atom by ca. 3.6° for **2a** and 5.2° for **2b**. In contrast, indenyl ligands in [Co(η^5-indenyl)$_2$]$^+$ are folded away from the cobalt atom that is caused by steric repulsion [11b]. In the case of **2a**, distances from the rhodium atom to planes of the C_5 ring of indenyl ligands Rh···C_5 (av. 1.820 Å) are longer than Rh···Cp distances in [$RhCp_2$]$^+$ (av. 1.808 Å) [21], suggesting weaker bonding of rhodium with the indenyl ligand than with Cp.

In both cations indenyl ligands have fully eclipsed mutual conformation, in which the bridgehead carbon atoms of the indenyl ligands are arranged close to each other (Fig. 4). The same pattern was observed earlier for (indenyl)rhoda- and iridacarboranes and explained by *trans* effect and the symmetry of molecular orbitals of indenyl and carborane ligands [22]. Interestingly, the replacement of rhodium or iridium by cobalt leads to displacement of the mutual orientation of the indenyl ligands to the nearest staggered conformation which is realized in [Co(η^5-indenyl)$_2$]$^+$ [11b]. The conformational change may be explained by increase of steric repulsion due to shortening of the distance between indenyl ligands (av. 3.32 Å for [Co(η^5-indenyl)$_2$]$^+$ *vs.* 3.66 Å for **2a** and 3.56 Å for **2b**).

3. Conclusion

The reactions of iodide complexes [(η^5-indenyl)MI_2]$_n$ (M = Rh, Ir; **1a**,**b**) with indenes in the presence of silver salts have been shown to be an effective approach for the synthesis of bis(indenyl)-rhodium and -iridium complexes. The reaction does not tolerate bulky substituents in the incoming indene. Cations [M(η^5-indenyl)$_2$]$^+$ (M = Rh, Ir; **2a**,**b**) were synthesized and structural characterized for the first time. In the solid state they have fully eclipsed conformation of indenyl ligands.

4. Experimental section

The reactions were carried out under an inert atmosphere in dry solvents. The isolation of products was conducted in air. Starting materials **1a** [5b], **1b** [16], and 1,2,3,4,7-pentamethylindene [23] were prepared as described in the literature. ^{1}H and ^{13}C{^{1}H} NMR

Table 1
Results of energy decomposition analysis (energy values in kcal mol^{-1}) for cations [M(η^5-indenyl)$_2$]$^+$ (M = Co, Rh, Ir) using [(η^5-indenyl)M]$^{2+}$ and [indenyl]$^-$ as interacting fragments at the BP86/TZP level.

M	ΔE_{int}	ΔE_{Pauli}	$\Delta E^{[a]}_{elstat}$	$\Delta E^{[a]}_{orb}$	ΔE_{prep}	D_e
Co	−333.49	148.57	−276.03 (57.3%)	−206.04 (42.7%)	3.08	330.41
Rh (**2a**)	−317.20	170.72	−281.33 (57.7%)	−206.59 (42.3%)	4.06	313.14
Ir (**2b**)	−346.26	236.90	−329.57 (56.5%)	−253.59 (43.5%)	5.29	340.97

[a] The values in parentheses give the percentage contribution to the total attractive interactions.

Table 2
Calculated (at the BP86/TZP level) and experimental (in acetone-d_6) ^{13}C NMR chemical shifts for cations [M(η^5-indenyl)$_2$]$^+$ (M = Co, Rh, Ir).

M	C1/3	C2	C8/9	C4/7	C5/6
Co	74.1	76.5	101.8	122.1	131.2
	76.7	*83.0*	*98.3*	*122.8*	*130.7*
Rh (**2a**)	78.4	81.2	107.8	121.3	131.2
	79.7	*85.8*	*101.9*	*120.6*	*128.4*
Ir (**2b**)	69.9	73.1	100.2	120.8	130.6
	72.1	*78.3*	*96.8*	*120.1*	*128.3*

[a] The calculated chemical shifts are shown in normal type and experimental values in italics.

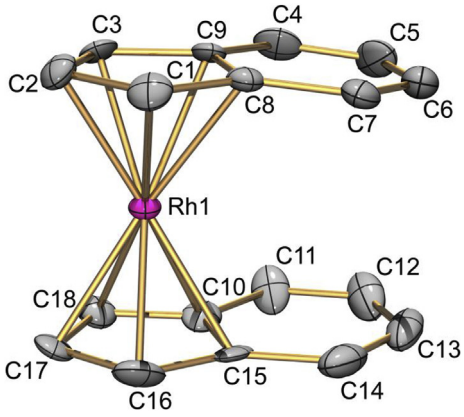

Fig. 2. Structure of cation **2a**. Ellipsoids are shown at the 50% level. Hydrogen atoms are omitted for clarity. Selected bond lengths (Å): Rh1–C1 2.187(6), Rh1–C2 2.161(6), Rh1–C3 2.163(6), Rh1–C8 2.211(6), Rh1–C9 2.217(5), Rh1–C10 2.219(6), Rh1–C15 2.209(6), Rh1–C16 2.172(6), Rh1–C17 2.169(6), Rh1–C18 2.176(6), C1–C2 1.429(9), C2–C3 1.417(9), C1–C8 1.425(9), C3–C9 1.438(9), C8–C9 1.446(9), C16–C17 1.419(10), C17–C18 1.424(9), C10–C18 1.422(9), C15–C16 1.433(10), C10–C15 1.441(9).

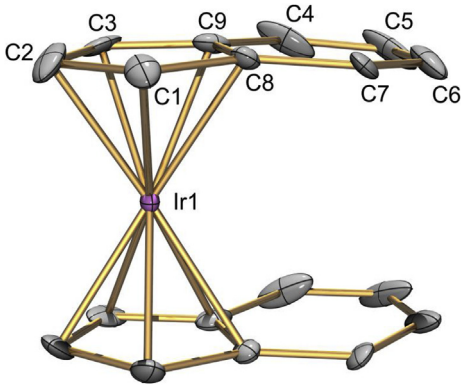

Fig. 3. Structure of cation **2b**. Ellipsoids are shown at the 30% level. Hydrogen atoms are omitted for clarity. Selected bond lengths (Å): Ir1–C1 2.189(15), Ir1–C2 2.149(14), Ir1–C3 2.169(14), Ir1–C8 2.222(14), Ir1–C9 2.220(13), C1–C2 1.47(3), C2–C3 1.47(2), C1–C8 1.43(2), C3–C9 1.45(2), C8–C9 1.433(19).

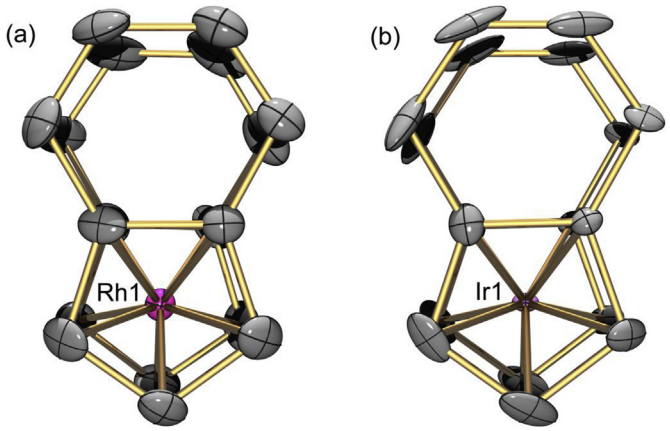

Fig. 4. Projections perpendicular to the indenyl ligand for the bis(indenyl) complexes **2a** (a) and **2b** (b).

spectra (δ in ppm) were recorded on a Bruker Avance-400 spectrometer operating at 400.13 and 100.61 MHz, respectively. The signals of the carbon atoms of the indenyl ligand in the ^{13}C NMR spectra were assigned by analogy with the (indenyl)iron complexes according to conventional numbering scheme [24].

*4.1. Synthesis of [(η^5-indenyl)Rh(η^5-$C_9H_2R_5$)]PF_6 (**2a**PF_6: R = H; **3**PF_6: R = Me)*

$MeNO_2$ (2 ml) was added to a mixture of **1a** (57 mg, 0.121 mmol), $AgPF_6$ (68.4 mg, 0.242) and indene or 1,2,3,4,7-pentamethylindene (0.242 mmol). The reaction mixture was stirred for 1 h. The precipitate of AgI was centrifugated off. The solvent was removed in vacuo and the residue was filtered in acetone through a layer of Al_2O_3 (15 cm). The solvent was removed in vacuo and the residue was reprecipitated by ether from acetone. Complexes **2a**PF_6 and **3**PF_6 were obtained as orange solids.

2aPF_6, R = H, yield 42 mg (73%). Anal. Calc. for $C_{18}H_{14}F_6PRh$: C, 38.00; H, 2.48. Found: C, 38.27; H, 2.36. ^{1}H NMR (acetone-d_6): δ = 7.41 (m, 2H, C_9H_7), 6.78 (m, 2H, C_9H_7), 6.33 (m, 2H, C_9H_7), 6.13 (m, 1H, C_9H_7). ^{13}C{^{1}H} NMR (acetone-d_6): δ = 128.4 (s, C5/6), 120.6 (s, C4/7), 101.9 (d, J_{Rh-C} = 6.0 Hz, C8/9), 85.8 (d, J_{Rh-C} = 8.0 Hz, C2), 79.7 (d, J_{Rh-C} = 8.0 Hz, C1/3).

3PF_6, R = Me, yield 26 mg (33%). Anal. Calc. for $C_{23}H_{24}F_6PRh$: C, 50.38; H, 4.41. Found: C, 50.26; H, 4.57. ^{1}H NMR (acetone-d_6): δ = 7.54 (m, 2H, C_9H_7), 7.23 (m, 2H, C_9H_7), 7.06 (s, 2H, $C_9\underline{H}_2Me_5$), 6.09 (m, 2H, C_9H_7), 6.0 (m, 1H, C_9H_7), 2.35 (s, 12H, $C_9H_2\underline{Me}_5$), 2.24 (s, 3H, $C_9H_2\underline{Me}_5$). ^{13}C{^{1}H} NMR (acetone-d_6): δ = 130.5 (s, C4/7, $C_9H_2Me_5$), 129.4 (s, C5/6, $C_9H_2Me_5$), 128.7 (s, C4/7, C_9H_7), 121.0 (s, C5/6, C_9H_7), 104.1 (d, J_{Rh-C} = 8.0 Hz, C2, $C_9H_2Me_5$), 102.1 (d, J_{Rh-C} = 6.0 Hz, C8/9, C_9H_7), 99.6 (d, J_{Rh-C} = 7.0 Hz, C8/9, $C_9H_2Me_5$), 95.1 (d, J_{Rh-C} = 8.0 Hz, C1/3, $C_9H_2Me_5$), 89.2 (d, J_{Rh-C} = 8.0 Hz, C2, C_9H_7), 81.7 (d, J_{Rh-C} = 8.0 Hz, C1/3, C_9H_7), 19.7 (s, $C_9H_2\underline{Me}_5$), 11.4 (s, $C_9H_2\underline{Me}_5$), 9.6 (s, $C_9H_2\underline{Me}_5$).

4.2. Synthesis of [Ir(η^5-indenyl)$_2$]PF_6 (**2b**PF_6)

$MeNO_2$ (2 ml) was added to a mixture of **1b** (60 mg, 0.107 mmol), $AgPF_6$ (61 mg, 0.214) and indene (0.028 ml, 0.242 mmol). The reaction mixture was stirred for 1 h. The precipitate of AgI was centrifugated off. The solvent was removed in vacuo and the residue was filtered in acetone through a layer of Al_2O_3 (15 cm). The solvent was removed in vacuo and the residue was reprecipitated by ether from acetone. Complex **2b**PF_6 was obtained as a pale yellow solid (46 mg, 75%). Anal. Calc. for $C_{18}H_{14}F_6IrP$: C, 38.10; H, 2.49. Found: C, 38.09; H, 2.57. ^{1}H NMR (acetone-d_6): $\delta = 7.30$ (m, 2H, C_9H_7), 6.78 (m, 2H, C_9H_7), 6.41 (d, J = 2.4 Hz, 2H, C_9H_7), 6.15 (t, J = 2.4 Hz, 1H, C_9H_7). $^{13}C\{^1H\}$ NMR (acetone-d_6): $\delta = 128.3$ (s, C5/6), 120.1 (s, C4/7), 96.8 (s, C8/9), 78.3 (s, C2), 72.1 (s, C1/3).

4.3. X-ray crystallography

Crystals of **2a**SbF_6 and **2b**PF_6 (the former with one molecule of acetone per two formula moieties of a complex) were obtained by slow diffusion in a two-layer system, ether or petroleum ether and a solution of complex in acetone. Complex **2a**SbF_6 was synthesized by the standard procedure using of $AgSbF_6$ instead of $AgPF_6$. X-ray diffraction data were collected with APEX2 DUO CCD diffractometer, using graphite monochromated Mo-Kα radiation (λ = 0.71073 Å, ω-scans) at 120 K. The structures were solved by direct method and refined by the full-matrix least-squares technique against F^2 in the anisotropic-isotropic approximation. Positions of hydrogen atoms were calculated, and they were refined in the isotropic approximation within the riding model. All calculations were performed using SHELXTL PLUS 5.0 [25]. Experimental details and crystal parameters are listed in Table 3.

4.4. Computational details

The geometries have been optimized without constraints at the gradient corrected DFT level of theory using the exchange functional of Becke [26] and the correlation functional of Perdew [27] (BP86). All-electron triple-ζ basis set augmented by one polarization function TZP was used. The bonding interactions were studied by means of Morokuma-Ziegler energy decomposition analysis [28]. The ^{13}C NMR shifts were calculated by subtraction of calculated isotropic shielding values from those of $[CoCp_2]^+$ (91.51 ppm at BP86/TZP; 85.72 ppm in acetone-d_6) [29]. The calculations were carried out using the ADF 2010.01 program package.

Table 3
Crystallographic data and structure refinement parameters for **2a**SbF_6 and **2b**PF_6.

Compound	**2a**SbF_6	**2b**PF_6
Empirical formula	$(C_{18}H_{14}Rh)_2(F_6Sb)_2\cdot C_3H_6O$	$C_{18}H_{14}IrPF_6$
Molecular weight	1195.98	567.46
Crystal system	Triclinic	Monoclinic
Space group	*P-1*	*C2/m*
a (Å)	9.1022(19)	12.725(3)
b (Å)	11.062(2)	12.572(3)
c (Å)	11.421(2)	10.434(3)
α (deg)	62.036(3)	90
β (deg)	75.568(4)	93.588(8)
γ (deg)	69.428(4)	90
V (Å^3)	946.0(3)	1666.0(8)
Z	1	4
D_{calcd} (g cm^{-3})	2.099	2.262
2_{max} (deg)	56	52
(Mo-*K*) (cm^{-3})	23.62	81.72
Collected reflections	10746	7901
Independent reflections	4568 (R_{int} = 0.0773)	1709 (R_{int} = 0.0401)
Observed reflections ($I > 2(I)$)	3250	1614
Parameters	262	132
R_1 (on *F* for obs. refls)	0.0475	0.0715
wR_2 (on F^2 for all refls)	0.1200	0.1873
F(000)	576	1072
GOF	0.990	1.624
Largest diff. peak and hole (e Å^{-3})	2.549 and −1.509	7.299 and −4.644

Acknowledgements

This work was supported by Russian Foundation for Basic Research (grant # 16-33-60140 mol_a_dk). The contribution of the Center of molecular composition studies of INEOS RAS is gratefully acknowledged.

Appendix A. Supplementary data

Supplementary data to this article can be found online at https://doi.org/10.1016/j.jorganchem.2018.11.027.

References

[1] B.M. Trost, M.C. Ryan, Angew. Chem. Int. Ed. 56 (2017) 2862–2879.
[2] a) A. Borrini, P. Diversi, G. Ingrosso, A. Luccherini, G. Serra, J. Mol. Catal. 30 (1985) 181–195;
b) A. Ceccon, A. Gambaro, S. Santi, A. Venzo, J. Mol. Catal. 69 (1991). Ll–L6;
c) L. Orian, M. Swart, F.M. Bickelhaupt, ChemPhysChem 15 (2014) 219–228.
[3] P. Smoleński, J. Organomet. Chem. 696 (2011) 3867–3872.
[4] J.A. Brinkman, T.T. Nguyen, J.R. Sowa, Org. Lett. 2 (2000) 981–983.
[5] a) A.P. Moskovets, D.L. Usanov, O.I. Afanasyev, V.A. Fastovskiy, A.P. Molotkov, K.M. Muratov, G.L. Denisov, S.S. Zlotskii, A.F. Smol'yakov, D.A. Loginov, D. Chusov, Org. Biomol. Chem. 15 (2017) 6384–6387;
b) S.A. Runikhina, M.A. Arsenov, V.B. Kharitonov, E.R. Sovdagarova, O. Chusova, Y.V. Nelyubina, G.L. Denisov, D.L. Usanov, D. Chusov, D.A. Loginov, J. Organomet. Chem. 867 (2018) 106–112;
c) V.B. Kharitonov, M. Makarova, M.A. Arsenov, Y.V. Nelyubina, O. Chusova, A.S. Peregudov, S.S. Zlotskii, D. Chusov, D.A. Loginov, Organometallics 37 (2018) 2553–2562.
[6] a) D.A. Loginov, V.E. Konoplev, J. Organomet. Chem. 867 (2018) 14–24;
b) J. Terasawa, Y. Shibata, Y. Kimura, K. Tanaka, Chem. Asian J. 13 (2018) 505–509;
c) N. Semakul, K.E. Jackson, R.S. Paton, T. Rovis, Chem. Sci. 8 (2017) 1015–1020;
d) T. Piou, F. Romanov-Michailidis, M. Romanova-Michaelides, K.E. Jackson, N. Semakul, T.D. Taggart, B.S. Newell, C.D. Rithner, R.S. Paton, T. Rovis, J. Am. Chem. Soc. 139 (2017) 1296–1310;
e) D.A. Loginov, A.O. Belova, A.R. Kudinov, Russ. Chem. Bull. 63 (2014) 983–986.
[7] A. Hart-Davis, R.J. Mawby, J. Chem. Soc. A (1969) 2403–2407.
[8] a) T.J. Kealy, P.L. Pauson, Nature 168 (1951) 1039–1040;
b) G.B. Kauffman, J. Chem. Educ. 60 (1983) 185–186.
[9] F.A. Cotton, R.O. Whipple, G. Wilkinson, J. Am. Chem. Soc. 75 (1953) 3586–3587.
[10] a) P.L. Pauson, G. Wilkinson, J. Am. Chem. Soc. 76 (1954) 2024–2026;
b) J. Trotter, Acta Crystallogr. 11 (1958) 355–360;
c) S.A. Westcott, A.K. Kakkar, G. Stringer, N.J. Taylor, T.B. Marder, J. Organomet. Chem. 394 (1990) 777–794;
d) O.J. Curnow, G.M. Fern, J. Organomet. Chem. 690 (2005) 3018–3026;
e) M. Maekawa, C.G. Daniliuc, M. Freytag, P.G. Jones, M.D. Walter, Dalton Trans. 41 (2012) 10317–10327.
[11] a) D. O'Hare, V.J. Murphy, N. Kaltsoyannis, J. Chem. Soc., Dalton Trans. (1993) 383–392;
b) D. Bellamy, N.G. Connelly, G.R. Lewis, A.G. Orpen, CrystEngComm 4 (2002) 68–79;
c) P. Ransom, A. Ashley, A. Thompson, D. O'Hare, J. Organomet. Chem. 694 (2009) 1059–1068.
[12] H.P. Fritz, F.H. Köhler, K.E. Schwarzhans, J. Organomet. Chem. 19 (1969) 449–452.
[13] a) N.C. Webb, R.E. Marsh, Acta Crystallogr. 22 (1967) 382–387;
b) N.C. Crossley, J.C. Green, A. Nagy, G. Stringer, J. Chem. Soc., Dalton Trans. (1989) 2139–2147;
c) A.A. Titov, A.F. Smol'yakov, O.A. Filippov, I.A. Godovikov, D.A. Muratov, F.M. Dolgushin, L.M. Epstein, E.S. Shubina, Cryst. Growth Des. 17 (2017) 6770–6779.
[14] S.V. Kukharenko, V.V. Strelets, L.I. Denisovich, M.G. Peterleitner, A.Z. Kreindlin, A.R. Kudinov, M.I. Rybinskaya, Russ. Chem. Bull. 44 (1995) 2289–2294.
[15] Z.G. Lewis, A.J. Welch, J. Organomet. Chem. 438 (1992) 353–369.
[16] A.A. Chamkin, A.M. Finogenova, Yu V. Nelyubina, J. Laskova, A.R. Kudinov,

D.A. Loginov, Mendeleev Commun. 26 (2016) 491–493.
[17] C. White, S.J. Thompson, P.M. Maitlis, J. Chem. Soc., Dalton Trans. (1977) 1654–1661.
[18] F.H. Kohler, Chem. Ber. 107 (1974) 570–574.
[19] The dissociation energies (D_e) were estimated by energy decomposition analysis: a) G. Frenking, J. Organomet. Chem. 635 (2001) 9–23;
b) G. Frenking, K. Wichmann, N. Fröhlich, C. Loschen, M. Lein, J. Frunzke, V.M. Rayon, Coord. Chem. Rev. 238 (2003) 55–82;
c) G. Frenking, A. Krapp, J. Comput. Chem. 28 (2007) 15–24;
d) T. Ziegler, J. Autschbach, Chem. Rev. 105 (2005) 2695–2722;
e) M.J.S. Phipps, T. Fox, C.S. Tautermann, C.-K. Skylaris, Chem. Soc. Rev. 44 (2015) 3177–3211.
[20] Slip parameter is defined as difference in the average distances from metal to the bridgehead carbons and from metal to the adjacent carbon atoms: C. Sui-Seng, G.D. Enright, D. Zargarian Organometallics 23 (2004) 1236–1246.
[21] B. Klingert, G. Rihs, J. Inclusion Phenom. Mol. Recognit. Chem. 10 (1991) 255–265.
[22] a) D.A. Loginov, V.O. Idrisov, YuV. Nelyubina, YuN. Laskova, A.R. Kudinov, Russ. Chem. Bull. 66 (2017) 346–349;
b) M.A. Arsenov, V.B. Kharitonov, E.R. Sovdagarova, A.F. Smol'yakov, D.A. Loginov, J. Organomet. Chem. 865 (2018) 45–50.
[23] D.A. Loginov, M.M. Vinogradov, Z.A. Starikova, E.A. Petrovskaya, P. Zanello, F. Laschi, F. Rossi, A. Cinquantini, A.R. Kudinov, J. Organomet. Chem. 692 (2007) 5777–5787.
[24] D.A. Loginov, A.A. Chamkin, V.B. Kharitonov, E.R. Sovdagarova, Y.V. Nelyubina, A.R. Kudinov, ChemistrySelect 2 (2017) 3549–3556.
[25] G.M. Sheldrick, Acta Crystallogr. A 64 (2008) 112–122.
[26] A.D. Becke, Phys. Rev. A 38 (1988) 3098–3100.
[27] J.P. Perdew, Phys. Rev. B 33 (1986) 8822–8824.
[28] a) K. Morokuma, Chem. Phys. 55 (1971) 1236–1244;
b) T. Ziegler, A. Rauk, Theor. Chim. Acta 46 (1977) 1–10.
[29] R.B. Materikova, V.N. Babin, I.R. Lyatifov, R.M. Salimov, E.I. Fedin, P.V. Petrovskii, J. Organomet. Chem. 219 (1981) 259–267.